SLAC-PUB-14892
March 2012

INTRA-BEAM SCATTERING, IMPEDANCE, AND INSTABILITIES IN ULTIMATE STORAGE RINGS*

K.L.F. Bane,
SLAC National Accelerator Laboratory, Stanford, CA 94309, USA

*Presented at the ICFA Workshop on Future Light Sources: FLS2012,
Thomas Jefferson National Accelerator Facility, Newport News, VA, 5–9 March 2012*

*Work supported by Department of Energy contract DE–AC02–76SF00515.

INTRA-BEAM SCATTERING, IMPEDANCE, AND INSTABILITIES IN ULTIMATE STORAGE RINGS*

K.L.F. Bane, SLAC, Menlo Park, CA 94025, USA

Abstract

We have investigated collective effects in an ultimate storage ring, *i.e.* one with diffraction limited emittances in both planes, using PEP-X as an example. In an ultimate ring intra-beam scattering (IBS) sets the limit of current that can be stored. In PEP-X, a 4.5 GeV ring running round beams at 200 mA in 3300 bunches, IBS doubles the emittances to 11.5 pm at the design current. The Touschek lifetime is 11 hours. Impedance driven collective effects tend not to be important since the beam current is relatively low.

INTRODUCTION

Recently there has been a growing interest in the idea of an "ultimate" storage ring, *i.e.* one with diffraction limited emittances, at one angstrom wavelength, in both planes [1]. One such design is PEP-X, a 4.5 GeV machine that fits into the PEP-II tunnel at SLAC [2]. PEP-X uses a unique nonlinear optimization scheme, resulting in an ultimate ring with tolerances that are challenging but achievable.

A previous PEP-X design, so-called "baseline" PEP-X [3], used a different lattice, and achieved an emittance that was diffraction limited in the vertical (8 pm) but not in the horizontal (160 pm). However, for ultimate PEP-X the beam current is much reduced (0.2 A instead of 1.5 A) and the beams are taken to be round, with equal horizontal and vertical emittances. In the design report for baseline PEP-X the collective effects of intra-beam scattering (IBS), Touschek lifetime, and impedance-driven instabilities were studied in some detail. It was found, for example, that IBS and Touschek were limiting effects, and that the multi-bunch tranverse instability required a feedback system that is challenging.

In this report we study IBS, Touschek lifetime, and impedance-driven instabilities in the ultimate storage ring version of PEP-X. For details on other aspects of the PEP-X project design, the reader is referred to Y. Cai's report for this conference [4]. A selection of PEP-X parameters used in this report is given in Table 1.

Table 1: A selection of PEP-X parameters. Note that the nominal horizontal emittance $\epsilon_{x0} = \epsilon_0/(1+\kappa)$.

Parameter	Value	Units
Energy, E	4.5	GeV
Circumference, C	2199.	m
Average current, I	200	mA
Bunch population, N_b	2.8	10^9
Number of bunches, M	3300	
Relative rms energy spread, σ_{p0}	1.1	10^{-3}
Rms bunch length, σ_{z0}	3.0	mm
Nominal emittance sum, ϵ_0	10.95	pm
$x-y$ coupling parameter, κ	1	
Momentum compaction, α	4.96	10^{-5}
Vertical tune, fractional part, $[\nu_y]$	0.14	
Synchrotron tune, ν_s	6.9	10^{-3}
Horiz. radiation damping time, τ_x	19.1	ms
Vert. radiation damping time, τ_y	22.5	ms
Long. radiation damping time, τ_p	12.3	ms

INTRA-BEAM SCATTERING

Intra-beam scattering describes multiple Coulomb scattering that in electron machines leads to an increase in all bunch dimensions and in energy spread, whereas the Touschek effect concerns large single Coulomb scattering events where energy transfer from transverse to longitudinal leads to immediate particle loss. In low emittance machines, such as PEP-X, both effects tend to be important.

For PEP-X IBS calculations we employ the Bjorken-Mtingwa (B-M) formulation [5], using the Nagaitsev [6] algorithm for efficient calculation. We assume that we are coupling dominated, by which we imply that the vertical dispersion can be kept sufficiently small. Then the vertical emittance is proportional to the horizontal emittance, and we write

$$\epsilon_x = \frac{\epsilon}{1+\kappa} \qquad \text{and} \qquad \epsilon_y = \frac{\kappa\epsilon}{1+\kappa}\,, \tag{1}$$

with κ the coupling constant and ϵ the sum emittance. The nominal (no IBS) horizontal and vertical emittances are given by $\epsilon_{x0} = \epsilon_0/(1+\kappa)$ and $\epsilon_{y0} = \kappa\epsilon_0/(1+\kappa)$, where ϵ_0 is a property of the lattice.

We make the assumption that the transverse growth rate can be approximated

$$\frac{\epsilon_{x0}}{\tau_x} + \frac{\epsilon_{y0}}{\tau_y} - \frac{\epsilon_x}{\tau_x} - \frac{\epsilon_y}{\tau_y} + \frac{\epsilon_x}{T_x} = 0\,, \tag{2}$$

where τ_x, τ_y, signify the radiation damping times in x, y, and $1/T_x$ gives the IBS growth rate *in amplitude* (the growth rate in emittance is just $2/T_x$). The first two terms in Eq. 2 represent quantum excitation growth rates, the next two terms those of radiation damping, and the last term that of IBS. (A similar equation applies for the growth in p.) Then IBS calculations of the steady-state emittance ϵ and (relative) energy spread σ_p are performed by simulta-

* Work supported by Department of Energy contract DE–AC02–76SF00515.

neously solving

$$\epsilon = \frac{\epsilon_0}{1-\tau_x^*/T_x} \qquad \text{and} \qquad \sigma_p^2 = \frac{\sigma_{p0}^2}{1-\tau_p/T_p}\ , \tag{3}$$

where $\tau_x^* = \tau_x/(1+\kappa\tau_x/\tau_y)$. The quantities σ_{p0}, τ_p, and $1/T_p$ signify, respectively, the nominal beam size, the radiation damping time, and the IBS growth rate in p.

B-M gives the local growth rates $\delta(1/T_x)$, $\delta(1/T_p)$, in terms of beam properties and local lattice properties. These rates are calculated for all positions around the ring and then averaged ($\langle\rangle$ means to average around the ring) to give $\langle\delta(1/T_x)\rangle = 1/T_x$, $\langle\delta(1/T_p)\rangle = 1/T_p$, and then Eqs. 3 are solved simultaneously. Note that since the growth rates also depend on the beam emittances, energy spread, and bunch length Eqs. 3 need to be solved by iteration.

A simplified model of the B-M equations that can be used (with slight modification) to approximate the results for PEP-X is the so-called "high energy approximation" [7]. We present it here since it may more clearly show the parameter dependence of IBS than the B-M equations, though to obtain the numerical results for PEP-X (given below) we will use the more accurate B-M equations. According to this simplified model the IBS growth rate in energy spread is given by

$$\frac{1}{T_p} \approx \frac{r_e^2 c N_b (\log)}{16\gamma^3 \epsilon_x^{3/4}\epsilon_y^{3/4}\sigma_z\sigma_p^3}\left\langle \sigma_H\, g(a/b)\ (\beta_x\beta_y)^{-1/4}\right\rangle\ . \tag{4}$$

Here r_e is the radius of the electron, c the speed of light, N_b the number of electrons per bunch, $(\log)$ the Coulomb log factor, γ the Lorentz energy factor, σ_z the bunch length, and β_x, β_y, the optical beta functions. Other factors in Eq. 4 are defined by

$$\frac{1}{\sigma_H^2} = \frac{1}{\sigma_p^2} + \frac{\mathcal{H}_x}{\epsilon_x}\ , \quad a = \frac{\sigma_H}{\gamma}\sqrt{\frac{\beta_x}{\epsilon_x}}\ , \quad b = \frac{\sigma_H}{\gamma}\sqrt{\frac{\beta_y}{\epsilon_y}}\ , \tag{5}$$

$$g(\alpha) = \alpha^{(0.021-0.044\ln\alpha)}\ , \tag{6}$$

where $\mathcal{H} = [\eta^2 + (\beta\eta' - \frac{1}{2}\beta'\eta)^2]/\beta$ is the dispersion invariant. Finally, the horizontal IBS growth rate (in amplitude) is given by

$$\frac{1}{T_x} = \frac{\sigma_p^2}{\epsilon_x}\langle\mathcal{H}_x\delta(1/T_p)\rangle \quad . \tag{7}$$

Note that Eq. 7 is slightly different than the corresponding equation given in Ref. [7], where it reads

$$\frac{1}{T_x} = \frac{\sigma_p^2}{\epsilon_x}\langle\mathcal{H}_x\rangle\frac{1}{T_p} \quad ; \tag{8}$$

that version was derived from the present version assuming no correlations between $\mathcal{H}_x$ and $\delta(1/T_p)$.* In the PEP-X lattice, however, these functions are anti-correlated in the arcs; for it we find reasonable agreement for the current version of the equation, while the earlier version is a factor of 2 larger. Finally, note that the high energy IBS approximation given here has validity when a, $b \ll 1$, which for PEP-X parameters holds.

In scattering calculations, like IBS, a Coulomb log term is used to take into account the contribution of very large and very small impact parameter events. Due to the very small impact parameter events the tails of the steady-state bunch distributions are not Gaussian and the standard way of computing $(\log)$ overemphasizes their importance. To better describe the size of the core of the bunch we calculate the Coulomb log factor as first proposed by Raubenheimer [8, 9]. For PEP-X, $(\log) \approx 11$.

For our IBS calculations nominal parameters are obtained from Table 1, and the lattice used is that described in Ref. [2]. We assume that potential well bunch lengthening is not significant and that the nominal current is below the threshold to the microwave instability. The beam runs on a coupling resonance, so that we have a round beam and $\kappa = 1$. The results of our B-M IBS calculations for PEP-X are shown in Table 2, where we give steady-state emittances, ϵ_x and ϵ_y, energy spread σ_p and bunch length σ_z. We note that for PEP-X, IBS has little effect on σ_p and σ_z; however, at the nominal current ϵ_x is double the zero-current value. We can see that it is IBS (and the goal of being diffraction limited in both planes) that sets the choices of $I = 200$ mA and round beams for PEP-X.

Table 2: For PEP-X: steady-state emittances, energy spread, and bunch length at zero and nominal currents.

I [mA]	ϵ_x [pm]	ϵ_y [pm]	σ_p [10^{-3}]	σ_z [mm]
0	5.5	5.5	1.10	3.00
200	11.5	11.5	1.15	3.15

At nominal current the horizontal IBS growth rate is $T_x^{-1} = 52\ \mathrm{s}^{-1}$ (and the energy growth rate $T_p^{-1} = 7.4\ \mathrm{s}^{-1}$). The accumulation around the ring of the horizontal growth rate is shown in Fig. 1. We note that, as expected, the growth rate is significant only in the arc regions, where there are bends and $\mathcal{H}_x$ is non-zero. Note also that from the high energy approximation, Eqs. 4, 7, we obtain $T_x^{-1} = 53.7\ \mathrm{s}^{-1}$ and $T_p^{-1} = 8.9\ \mathrm{s}^{-1}$, in reasonable agreement to the Bjorken-Mtingwa solution.

A comparison IBS calculation was performed using the optics program SAD [10]. We realize that our approach handles x-y coupling in an approximate manner. SAD treats coupling properly, by obtain *e.g.* the true emittance invariants, and it can also solve the B-M IBS equations. In the dispersion-free regions quad strengths were adjusted to bring the tunes close to each other. Then 800 quadrupole magnets in these regions were rotated by small random amounts, and adjusted by an overall scale factor to give $\epsilon_{x0} \approx \epsilon_{y0}$. Then IBS calculations were performed. The procedure was repeated for 10 seeds (for the random number generator), and the results varied only

*Eq. 8 was well-known before Ref. [7] and in fact can be found in B-M's report.

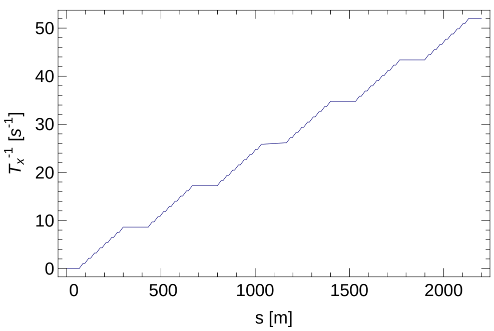

Figure 1: Accumulation around the ring of the IBS growth rate in x. The positions where the slope of the curve is nonzero are in the arcs.

by a small amount. The final result is that, with IBS, $\epsilon_x \approx \epsilon_y \approx 11$ pm, a result that is not far from our 11.5 pm.

We have calculated also the steady-state emittances as functions of beam current; the result is shown in Fig. 2 (the solid curve). In our calculations we have again observed that for PEP-X the growth of longitudinal emittance due to IBS is very small. This means that, to good approximation, σ_p and σ_z can be taken to have their nominal values and one need only solve the first of Eqs. 3. In this case we see from the simplified model that the horizontal emittance as function of current can be approximated by a solution (the maximum, real solution) of the equation

$$\left(\frac{\epsilon_x}{\epsilon_{x0}}\right)^{5/2} - \left(\frac{\epsilon_x}{\epsilon_{x0}}\right)^{3/2} = \alpha\left(\frac{I}{I_A}\right) \quad , \tag{9}$$

with α a constant and $I_A = 17$ kA the Alfvén current. Here the best fit is obtained with $\alpha = 3.2 \times 10^5$ (see Fig. 2, the dashes).

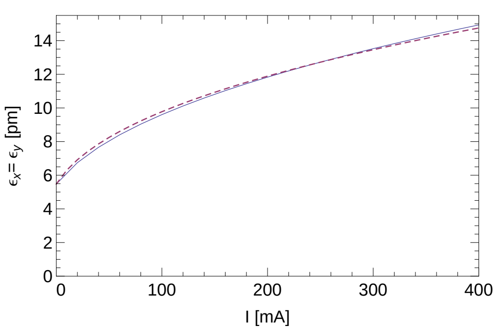

Figure 2: Steady-state emittances as function of bunch current in PEP-X.

Further IBS calculations were performed for the PEP-X lattice, but now allowing the energy of the machine to change through scaling. In Fig. 3 we plot emittance *vs.* machine energy, at zero current and near nominal current. At nominal current, at low energies IBS becomes stronger and at high energies synchrotron radiation becomes stronger, with the minimum emittance obtained at $E = 5$ GeV. We see that the PEP-X energy is near-optimal.

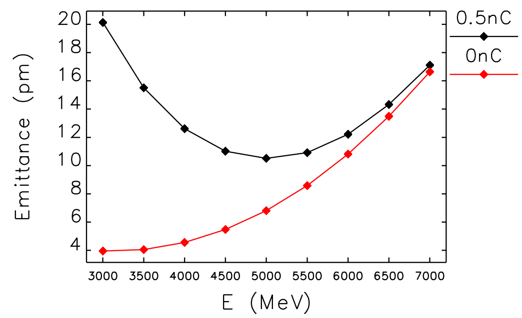

Figure 3: Emittance ϵ_x ($= \epsilon_y$) *vs.* energy E for the PEP-X lattice at nominal (black) and at zero (red) currents [2].

TOUSCHEK LIFETIME

Touschek lifetime calculations normally follow the flat-beam equation of Brück [11], with modifications by Piwinski [12]. For round beam calculations we here will begin with the more general formula (*i.e.* not limited to flat beams) due to Piwinski [12, 13]. With the Touschek effect the number of particles in a bunch decays with time t as

$$N_b = \frac{N_{b0}}{1 + t/\mathcal{T}} \ , \tag{10}$$

with N_{b0} the initial bunch population, and $\mathcal{T}$ the Touschek lifetime. Note that the decay is not exponential. The lifetime is given by [12]

$$\frac{1}{\mathcal{T}} = \frac{r_e^2 c N_b}{8\sqrt{\pi}\beta^2\gamma^4\sigma_z\sigma_p\epsilon_x\epsilon_y} \langle \sigma_H \mathcal{F}(\delta_m)\rangle \ , \tag{11}$$

with

$$\mathcal{F}(\delta_m) = \int_{\delta_m^2}^{\infty} \frac{d\tau}{\tau^{3/2}} e^{-\tau B_1} I_0(\tau B_2)\left[\frac{\tau}{\delta_m^2} - 1 - \frac{1}{2}\ln\left(\frac{\tau}{\delta_m^2}\right)\right] \tag{12}$$

$$B_{1,2} = \frac{1}{2\beta^2\gamma^2}\left|\frac{\beta_x\sigma_x^2}{\epsilon_x\tilde{\sigma}_x^2} \pm \frac{\beta_y}{\epsilon_y}\right| \ , \tag{13}$$

where again $\langle\rangle$ indicates averaging around the ring. In this formula the only assumptions are that there is no vertical dispersion and that the energies are non-relativistic in the beam rest frame ($\gamma^2\sigma_x^2/\beta_x^2$, $\gamma^2\sigma_y^2/\beta_y^2 \ll 1$); there is no requirement that the beam be flat. Parameters are average velocity over the speed of light β, modified Bessel function of the first kind I_0, relative momentum acceptance δ_m (half aperture), and beam sizes $\sigma_x = \sqrt{\beta_x\epsilon_x + \eta_x^2\sigma_p^2}$ and $\tilde{\sigma}_x = \sqrt{\beta_x\epsilon_x + \beta_x\mathcal{H}_x\sigma_p^2}$ (σ_H is defined in Eq. 5).

Because of the cut-off factor $\exp(-\tau B_1)$ in the integral of Eq. 12, with $B_1 \sim \beta/\epsilon$: (i) the Touschek effect is strongest where the beam size is small (in the arcs for PEP-X), and (ii) the effect becomes weak for very small emittances. For the special case of round beams we can do an approximate calculation, letting $B_1 = \beta_x \sigma_x^2/(\beta^2\gamma^2\epsilon_x\tilde{\sigma}_x^2)$ and $B_2 = 0$. For PEP-X this approximation yields a result that is within 10% of the more accurate result.

The Touschek lifetime depends on the momentum acceptance in the ring, and thus we have calculated the momentum acceptance due to first order optics as a function of location in PEP-X (see Fig. 4): In tracking, at a given position s a beam particle is given a relative (positive) momentum kick δ_m, and it undergoes betatron oscillation. The largest value of δ_m for which the particle survives defines the positive momentum aperture at position s. Then the same is done for a negative momentum kick. From the plot we see that the typical value of momentum acceptance for PEP-X (in the bends) is $\delta_m \sim \pm 2.8\%$.

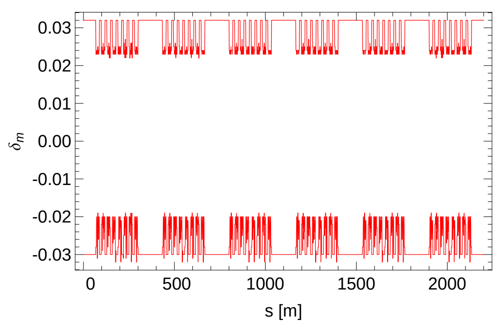

Figure 4: The momentum acceptance due to the linear optics, δ_m, for PEP-X [2]. This function is used in finding the Touschek lifetime.

Using the δ_m as shown in Fig. 4, the Touschek lifetime was calculated numerically for the case of PEP-X, yielding $\mathcal{T} = 11.6$ hours, which is quite ample for running a light source. Note that this calculation was based on the IBS determined, steady-state beam sizes. In Fig. 5 we plot the accumulation around the ring of the Touschek growth rate. We see from the plot that, as was the case for IBS, the Touschek effect is significant only in the arcs; here it is because the beam size is smaller there than in the straights.

To see the sensitivity of $\mathcal{T}$ to momentum acceptance, we have performed more calculations, but this time as a function of *global* acceptance parameter δ_m (with the momentum aperture everywhere given by $\pm\delta_m$) (see Fig. 6, the blue symbols). The curve in the plot gives a fit to the calculations: $\mathcal{T} = 0.088(\delta_m/0.01)^5$. We see that the Touschek lifetime is a very sensitive function of momentum aperture: at $\delta_m = 2\%$ the lifetime is only ~ 2 hrs.

The damping wigglers, of nominal length $L_w = 90$ m, reduce the emittance in PEP-X. In Fig. 7 we plot ϵ_x and $\mathcal{T}$ (normalized to their values when $L_w = 90$ m) *vs.* L_w (upper plot). We see that the emittance decreases and the lifetime increases (gradually; over most of the range) with increasing wiggler length. In the lower plot we display $\mathcal{T}$

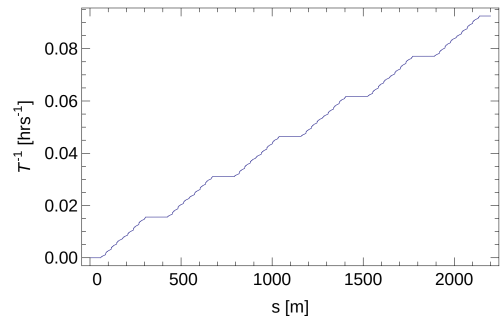

Figure 5: Accumulation around the ring of the Touschek growth rate in PEP-X configuration. The growth is significant only in the arcs.

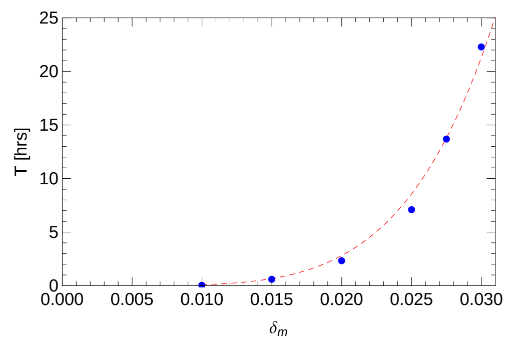

Figure 6: Touschek lifetime $\mathcal{T}$ *vs.* (global) momentum acceptance parameter, δ_m (blue symbols). The dashed curve gives the fit: $\mathcal{T} = 0.088(\delta_m/0.01)^5$.

vs. ϵ_x. We see that the lifetime increases with decreasing emittance in PEP-X, though relatively slowly.

IMPEDANCE AND INSTABILITIES

For the baseline design of PEP-X [3], an impedance budget was accumulated and calculations were performed on longitudinal and transverse instability thresholds and on growth rates. In the present report we again perform such calculations but go into less detail. We justify this by the fact that the present bunch current is a factor of 7.5 smaller than the previous one, and consequently instabilities are not such an important issue. We here briefly address three instabilities: (i) the single-bunch microwave instability excited by coherent synchrotron radiation (CSR), (ii) the single-bunch transverse mode coupling instability (TMCI) due to the resistance in the walls, and (iii) the multi-bunch transverse instability driven by the wall resistance.

Microwave Instability due to CSR

For the baseline design of PEP-X an impedance budget and single bunch wake representing the entire ring was gen-

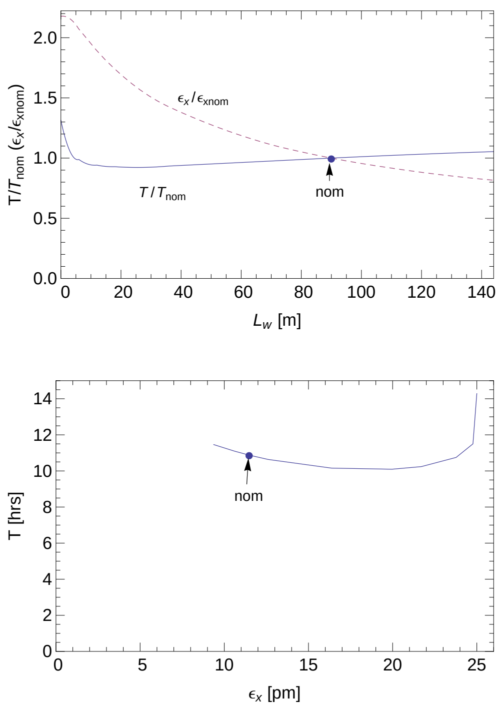

Figure 7: Emittance ϵ_x $(= \epsilon_y)$ and Touschek lifetime $\mathcal{T}$ *vs.* wiggler length L_w (upper plot) and $\mathcal{T}$ *vs.* ϵ_x (lower plot). These results are self-consistent calculations including IBS. The points labeled "nom" represent the nominal case, with $L_w = 90$ m.

erated. These were used to estimate the threshold of the microwave instability, which was found to be comfortably above the earlier design current of 1.5 A. Here we estimate the microwave threshold due only to one contributor to the impedance, shielded CSR. In the model used for the calculations the beam is assumed to be moving in a circle of radius ρ (in the plane $y = 0$) between two parallel plates at locations $y = \pm h$. In normalized units the threshold current S^{th} is given as a function of shielding parameter Π by [14]

$$S^{th} = 0.50 + 0.12\Pi \,, \tag{14}$$

with

$$S = \frac{eN_b\rho^{1/3}}{2\pi\nu_s\gamma\sigma_p\sigma_z^{4/3}} \,, \qquad \Pi = \frac{\sigma_z\rho^{1/2}}{h^{3/2}} \,. \tag{15}$$

The PEP-X vacuum chamber in the arcs is elliptical with axes $(b_x, b_y) = (30.0, 12.5)$ mm and bending radius $\rho = 100.8$ m; we let $h = 12.5$ mm in the calculations. With these assumptions we find that for PEP-X the shielding is significant, with $\Pi = 22.7$, the threshold bunch population $N_b^{th} = 4.9 \times 10^{10}$, and the threshold current $I^{th} = 3.6$ A—high above the design current. (Note that, even if we were to increase the aperture so that there is no shielding—$S^{th} = 0.50$, the threshold would be 0.58 A, significantly above the design current.)

Transverse Single Bunch Instability

In most light sources with regions of small aperture vacuum chambers, the resistive wall is the dominant contribution to the transverse, single-bunch instability. The kick factor—the average kick experienced over a bunch—for a Gaussian bunch passing through a round, resistive beam pipe is given by [15]

$$\kappa_y = (0.723)\frac{c}{\pi^{3/2}b^3}\sqrt{\frac{Z_0}{\sigma_z\sigma_c}} \,, \tag{16}$$

with b the radius of the pipe, $Z_0 = 377\ \Omega$, and σ_c the conductivity of the beam pipe. The single bunch threshold current is given by [16]

$$I_b^{th} \approx 0.7\frac{4\pi c\,\nu_s(E/e)}{\mathcal{C}}\frac{1}{\sum_i \ell_i\beta_{y,i}\kappa_{y,i}} \,, \tag{17}$$

with $\mathcal{C}$ the circumference of the ring. The multi-bunch threshold is $I^{th} = MI_b^{th}$, with M the number of bunches. Eq. (17) allows for several region types in the ring, each of total length ℓ, beta function β_y, and kick factor κ_y.

The five region types of PEP-X, and their beam pipes are described in Table 3. For the threshold calculation we use the information in the table, letting the vertical half-aperture be b; the conductivity of Al (Cu) is taken to be 3.5 $(5.9)\times10^7\ \Omega^{-1}\mathrm{m}^{-1}$. We see that the undulator and wiggler sections dominate because of their small vertical aperture. We find the threshold current is $I = 1.8$ A, comfortably above the nominal current.

Table 3: PEP-X beam pipe chamber types, giving total length, cross-sectional shape (elliptical [E], circular [C], or rectangular [R]), half-height in x and y, and average beta function. Note: the straights are divided into regular (r) and injection (i) types, and the first three table entries are of Al, the last two of Cu.

Type	Length [m]	Shape	(b_x, b_y) [mm]	$\langle\beta_y\rangle$ [m]
Arcs	1318	E	(30.0, 12.5)	7.0
Straights r	510	C	(48.0, 48.0)	15.6
Straights i	123	C	(48.0, 48.0)	60.0
Undulators	158	E	(25.0, 3.0)	2.8
Wigglers	90	R	(22.5, 4.0)	12.0

Multi-bunch Transverse Instability

The resistive wall impedance is often the dominant contributor to the transverse coupled bunch instability in storage rings. Assuming only this source of impedance, the growth rate of the instability can be estimated as [17]

$$\Gamma = \frac{c\,(I/I_A)}{4\gamma\sqrt{\mathcal{C}(1-[\nu_y])}}\langle\beta A\rangle \tag{18}$$

where

$$\langle\beta A\rangle = \frac{4}{\sqrt{\pi Z_0}}\sum_i \frac{\ell_i\beta_{y,i}}{b_i^3\sqrt{\sigma_{c,i}}} \,, \tag{19}$$

with $I_A = 17$ kA and $[\nu_y]$ is the fractional part of the vertical tune. Here the beam pipe is again assumed to be round with radius b.

For the growth rate calculation we again use the information in Table 3, letting the vertical half-aperture be b. Again the undulator and wiggler sections dominate due to the small vertical aperture. We find that the total growth rate $\Gamma = 1.4\ \mathrm{ms}^{-1}$, equivalent to a growth time of 99 turns, which should be not too difficult to control with feedback.

CONCLUSIONS

We have investigated collective effects in PEP-X, an ultimate storage ring, *i.e.* one with diffraction limited emittances (at one angstrom wavelength) in both planes. In an ultimate ring intra-beam scattering (IBS) sets the limit of current that can be stored. In PEP-X, IBS doubles the emittances to 11.5 pm at the design current of 200 mA, assuming round beams.

The Touschek lifetime is quite large in PEP-X, 11.6 hours, and—near the operating point—increases with decreasing emittance. It is, however, a very sensitive function of momentum acceptance. In an ultimate ring like PEP-X impedance driven collective effects tend not to be important since the beam current is relatively low.

Before ultimate PEP-X can be realized, the question of how to run a machine with round beams needs serious study. For example, in this report we assumed that the vertical emittance is coupling dominated. It may turn out that using vertical dispersion is a preferable way to generate round beams. The choice will affect IBS and the Touschek effect.

ACKNOWLEDGMENTS

The author thanks K. Kubo for performing SAD IBS calculations, M. Borland for performing *elegant* IBS calculations, and A. Xiao for discussions on IBS theory with coupling. He also thanks his SLAC co-workers on this project, Y. Cai, Y. Nosochkov, and M.-H. Wang.

REFERENCES

[1] M. Bei et al, Nucl. Inst. Meth. A **622**, 518 (2010).

[2] Y. Cai et al, "PEP-X: an ultimate storage ring based on fourth-order geometric achromats", SLAC-PUB-14785, December 2011.

[3] K. Bane et al, "A design report of the baseline for PEP-X", SLAC-PUB-13999, June 2010.

[4] Y. Cai, "Future synchrotron light sources based on ultimate storage rings," contributed to this conference.

[5] J.D. Bjorken and S.K. Mtingwa, Particle Accelerators, **13**, 115 (1983).

[6] S. Nagaitsev, Phys. Rev. ST-AB **8**, 064403 (2005).

[7] K. Bane, "A simplified model of intrabeam scattering," EPAC02, Paris, June 2002, WEPRI120, p. 1443.

[8] T. Raubenheimer, Particle Accelerators **45**, 111 (1994).

[9] K. Kubo and K. Oide, Phys. Rev. ST-AB **4**, 124401 (2001).

[10] SAD, optics program written by K. Oide.

[11] H. Brück, *Accelérateurs Circulaires de Particules; introduction à la théorie*, (Saclay, 1966).

[12] A. Piwinski, in *Handbook of Accelerator Physics*, 3rd Printing, (New Jersey: World Scientific, 2006) p. 142.

[13] A. Piwinski, "The Touschek effect in strong focusing storage rings", DESY 98-179, March 1999.

[14] K. Bane et al, Phys. Rev. ST-AB **13**, 104402 (2010).

[15] A. Chao and M. Tigner eds., *Handbook of Accelerator Physics*, 3rd Printing, (New Jersey: World Scientific, 2006) p. 230.

[16] S. Krinsky, "Simulation of Transverse Instabilities in the NSLS II Storage Ring", BNL-75019-2005-IR, September 2005.

[17] A. Wolski et al, "Configuration studies and recommendations for the ILC damping rings", LBNL 59449, February 2006.